

# Estimation of the breakup cross sections in ${}^6\text{He}+{}^{12}\text{C}$ reaction within high-energy approximation and microscopic optical potential

**E.V. Zemlyanaya, V.K. Lukyanov, K.V. Lukyanov**

Joint Institute for Nuclear Research, Dubna 141980, Russia

**Abstract.** The breakup cross sections in the reaction  ${}^6\text{He}+{}^{12}\text{C}$  are calculated at about 40 MeV/nucleon using the high-energy approximation (HEA) and with the help of microscopic optical potentials (OP) of interaction with the target nucleus  ${}^{12}\text{C}$  of the projectile nucleus fragments  ${}^4\text{He}$  and  $2n$ . Considering the di-neutron  $h=2n$  as a single particle the relative motion  $h\alpha$  wave function is estimated so that to explain both the separation energy of  $h$  in  ${}^6\text{He}$  and the rms radius of the latter. The stripping and absorption total cross sections are calculated and their sum is compared with the total reaction cross section obtained within a double-folding microscopic OP for the  ${}^6\text{He}+{}^{12}\text{C}$  scattering. It is concluded that the breakup cross sections contribute in about 50% of the total reaction cross section.

## Introduction

In recent calculations [1], the data on elastic scattering of  ${}^6\text{He}$  on  ${}^{12}\text{C}$  at comparably large energies 38.3 and 41.6 MeV/nucleon [2], [3] were studied using the microscopic optical potentials (OP) [4], whose depths of real and imaginary parts as well as the strength of the surface term were corrected by the three fitted re-normalization coefficients  $N_R$ ,  $N_I$  and  $N_I^{sf}$ . It was shown that because of the limited set of experimental data the ill-posed problem reveals itself, and therefore not one but the number of sets of adjusted  $N$ 's (and the respective OP's) were obtained, each characterized by fairly small  $\chi^2$  value. In this connection, the study of physics of the process is desirable, namely the search of details of mechanism of the  ${}^6\text{He}+{}^{12}\text{C}$  interaction in different channels. At this stage we intend to study constituents of a total reaction cross section  $\sigma_R$ , the breakup  $\sigma_b$  and absorption  $\sigma_a$  cross section, and compare them with  $\sigma_R$  obtained with the help of the aforementioned OP's in elastic channel.

## 1 The model of ${}^6\text{He}$

We consider the simplest breakup  $h\alpha$ -model of  ${}^6\text{He}$ , where it is suggested consisting of two clusters  ${}^4\text{He}$  and  $h$ , the correlated pair of neutrons  $h=2n$  (the sim-

ilar model was also treated in [3]). The interaction between clusters is taken to be a WS potential with the adjusted geometrical parameters  $R = 1.45 fm$ ,  $a = 0.3 fm$  and the depth  $V_0 = 28.3 Mev$  that reproduces the separation energy  $\varepsilon = 0.975 MeV$  of  $h$  and yields the  $r_{rms}$  radius  $2.62 fm$  of  ${}^6He$ . The obtained s-wave function  $\varphi_b(s)$  of relative motion of clusters defines the density distribution

$$\varrho_b(s) = |\varphi_b(s)|^2 = (1/4\pi)|\varphi_{l=0}(s)|^2 \quad (1)$$

and will be used for the further calculations of the ground state matrix elements of breakup processes. Figure 1 exhibits that  $\varrho_b(r)$ , normalized to 1, coincides fairly well with  $\varrho_L(s)$ , the nucleon density distribution of  ${}^6He$  obtained within the known large-scale shell-model [5] (LSSM-model) which also gives  $r_{rms} = 2.586 fm$ . Thus, we may apply the 2-cluster  $h\alpha$ -model for the further calculations of elastic and breakup cross sections.

## 2 Folding potentials

In the framework of the  $h\alpha$ -model of  ${}^6He$  one can estimate the  ${}^6He+{}^{12}C$  OP as folding of two OP's of interaction of clusters  $\alpha$  and  $h$  with  ${}^{12}C$ :

$$\begin{aligned} U_{HeC}^{(b)}(r) &= V^{DF(b)} + iW^{(b)} = \\ &= \int d^3s \varrho_b(s) \left\{ U_\alpha(\mathbf{r} - (2/3)\mathbf{s}) + U_h(\mathbf{r} + (1/3)\mathbf{s}) \right\} = \\ &= 2\pi \int_0^\infty \varrho_b(s) s^2 ds \int_{-1}^1 dx \left\{ U_\alpha \left( \sqrt{r^2 + (1/9)s^2 - r(2/3)sx} \right) + \right. \\ &\quad \left. + U_h \left( \sqrt{r^2 + (4/9)s^2 + r(4/3)sx} \right) \right\}. \end{aligned} \quad (2)$$

Here the  $h$ - ${}^{12}C$  potential is taken as the twice neutron- ${}^{12}C$  OP  $U_h = 2U_n$ . In turn, potentials  $U_\alpha$  and  $U_n$  are calculated within the microscopic hybrid model of OP [4]. In the latter, the double-folding (DF) real part  $V^{DF}$  is constructed as is done in [6], [7], while the imaginary part is derived using the optical limit of a Glauber theory. So, the real and imaginary parts of OP are as follows:

$$\begin{aligned} V^{DF}(r) &= V^D(r) + V^{EX}(r) = \int d^3s_p d^3s_t \left\{ \varrho_p(\mathbf{s}_p) \varrho_t(\mathbf{s}_t) v_{NN}^D(s) + \right. \\ &\quad \left. + \int d^3s_p d^3s_t \varrho_p(\mathbf{s}_p, \mathbf{s}_p + \mathbf{s}) \varrho_t(\mathbf{s}_t, \mathbf{s}_t - \mathbf{s}) v_{NN}^{EX}(s) \exp \left[ i\mathbf{K}(r) \cdot \frac{\mathbf{s}}{M} \right] \right\}, \end{aligned} \quad (3)$$

$$W^H(r) = -\frac{1}{2\pi^2} \frac{E}{k} \bar{\sigma}_N \int_0^\infty j_0(qr) \varrho_p(q) \varrho_t(q) f_N(q) q^2 dq. \quad (4)$$

Here  $p$  and  $t$  are related to the projectile and target nucleus,  $\mathbf{s} = \mathbf{r} + \mathbf{s}_t - \mathbf{s}_p$ ,  $M = A_p A_t / (A_p + A_t)$ ,  $K(r)$  is the local nucleus-nucleus momentum, and  $\bar{\sigma}_N$ , the total NN cross section, averaged over the isospins of colliding nuclei. The current calculations apply the  $v_{NN}$  effective Paris nucleon-nucleon CDM3Y6 potentials (for details see in [6], [7]). As to the density distributions we use the

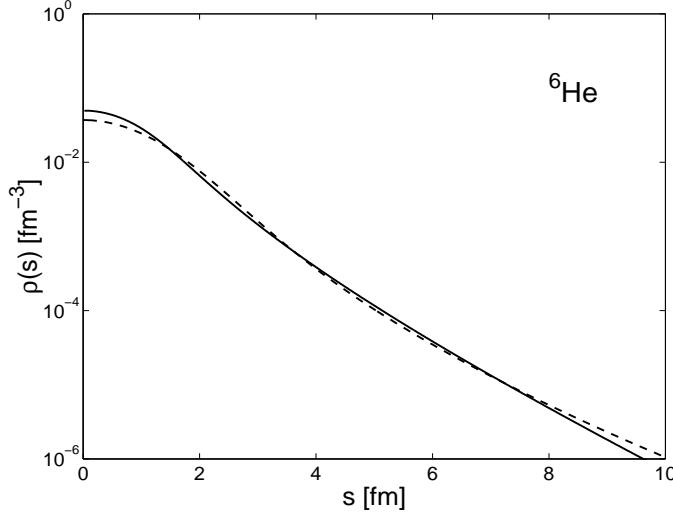


Figure 1. Comparison of the  $h\alpha$ -model density distribution  $\rho_b(s)$  (solid) with the LSSM density [5] (dashed).

two-parameter symmetrized fermi-densities  $\rho_p$  and  $\rho_t$  for nuclei  ${}^4\text{He}$  and  ${}^{12}\text{C}$  from [8]. Thus,  $U_\alpha$  and  $U_h = 2U_n$  OP's have the form

$$U_i(r) = V_i^{DF}(r) + iW_i(r), \quad i = \alpha, h, \quad (5)$$

where  $W(r)$  is either  $W^H(r)$  or  $V^{DF}(r)$ . Substituting OP's of fragments (5) in eq.(2), the respective real  $V^{DF(b)}$  and imaginary  $W^{(b)}$  parts of OP for  ${}^6\text{He}+{}^{12}\text{C}$  scattering are taken as results of folding with the  $h\alpha$ -model wave function. These parts are applied to construct the whole  ${}^6\text{He}+{}^{12}\text{C}$  OP as follows

$$U_{HeC}^{opt(b)} = N_R V^{DF(b)}(r) + iN_I W^{(b)}(r), \quad (6)$$

where the coefficients  $N_R$  and  $N_I$  are adjusted to get agreement with the respective experimental data on elastic scattering differential cross sections.

### 3 Elastic scattering

Doing so, we apply  $U_{HeC}^{opt(b)}(r)$  (6) to consider elastic scattering of  ${}^6\text{He}$  from  ${}^{12}\text{C}$  at  $E=38.3$  MeV/nucleon. In this case, there were applied two kinds of OP, with imaginary parts  $W=W^H(b)$  and  $W=V^{DF(b)}$ , and the corresponding differential cross sections were numerically calculated using the code DWUCK4 [9]. Besides, we compare these results with cross sections given in [1] where the entire double-folding OP (3) was utilized accounting for the LSSM density for  ${}^6\text{He}$  [5], and for the  ${}^{12}\text{C}$  density from [8]. Comparisons were made with the experimental

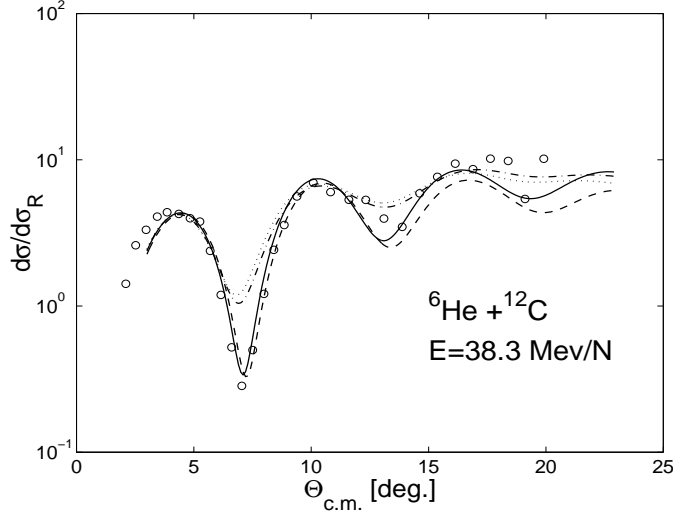


Figure 2. The  ${}^6\text{He}+{}^{12}\text{C}$  differential elastic cross sections at 38.3 MeV/N calculated using  $\rho_b$  density of the  $h\alpha$ -model for folding OP (eqs.(2),(6)): solid curve - for  $W^{(b)}=W^H(b)$ , dashed - for  $W^{(b)}=V^{DF}(b)$ . Dash-dotted and dotted curves are the entire double-folding calculations from [1] with the LSSM nucleon density of  ${}^6\text{He}$  and with  $W=V^{DF}$  and  $W=W^H$ , respectively (eqs.(3),(4)). The re-normalization  $N$ 's coefficients are in Table 1. Experimental data from [2].

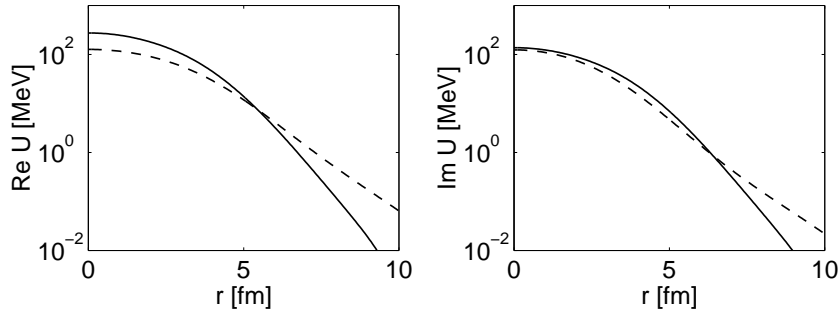


Figure 3. The  $h\alpha$ -model potential for  ${}^6\text{He}+{}^{12}\text{C}$  elastic scattering at  $E=38.3$  MeV/nucleon (solid) in comparison with the entire DF microscopic OP's applied in [1] (dashed). Left panel: real part; right panel: imaginary part.

data from [2]. The fitted re-normalization coefficients  $N$ 's are shown in Table 1. One can see from Fig.2 that angular distributions for different kinds of ImOP in the  $h\alpha$ -model (solid and dashed curves) as well as in the entire DF-model

### Estimation of the breakup cross sections in ${}^6\text{He}+{}^{12}\text{C}\dots$

Table 1. The adjusted  $\{N\}$  coefficients of OP and the DWUCK calculations within  $h\alpha$ - and DF-models for elastic cross sections in Fig.2.

potential	$N_R$	$N_I$	$\sigma_R^{tot}, \text{mb}$
$h\alpha$ -model, $N_R V^{DF(b)} + iN_I W^H(b)$ solid, eq.(6)	2.0	1.7	1018
$h\alpha$ -model, $N_R V^{DF(b)} + iN_I V^{DF(b)}$ dashed, eq.(6)	2.1	1.0	1042
entire DF-model, $N_R V^{DF} + iN_I W^H$ dotted, ref.[1]	1.268	0.511	1029
entire DF-model, $N_R V^{DF} + iN_I V^{DF}$ dash-dotted, ref.[1]	1.123	0.472	1034

(dash-dotted and dotted curves) are closely displayed, and the corresponding total reaction cross sections are almost equal in value as seen from Table 1. Also, Fig.3 shows the resulting  ${}^6\text{He}+{}^{12}\text{C}$  optical potentials, that correspond to the case of selection of the HEA  $ImOP$  (4) used in the  $h\alpha$ -model and in the entire DF-model. One sees that the  $ImOP$  for both models are rather similar. Nevertheless, we note that the sharper slope in the periphery of the  $h\alpha$ -model OP's leads to the pronounced angular distributions as compared to those calculated within the smooth DF-potential based on the  ${}^6\text{He}$  LSSM density. As a whole the  $h\alpha$ -model of  ${}^6\text{He}$  seems to be reliable for the further evaluations of total breakup cross sections, that is the subject of our study in the paper.

#### 4 Testing the HEA(eikonal) method

For calculations of breakup cross sections, the analytic eikonal (HEA) method is utilized. As to our further applications of HEA approach at energies of about 40 MeV/nucleon we should preliminary verify that this method is well working. For this purpose we calculate the notably characteristic of a process, the differential cross section of the  ${}^6\text{He}+{}^{12}\text{C}$  elastic scattering at 38.3 MeV/nucleon, within the numerical code DWUCK4 and also using the HEA method. In both cases we apply the same microscopic double-folding OP  $U^{opt} = (1.123 + i0.472)V^{DF}(r)$  from [1]. For this OP the exact result for the angular distribution was already shown in Fig.2 by the dashed-dotted curve. As to the analogical eikonal calculations we first exhibit the explicit expression for the HEA amplitude of scattering (for details see ref. [10])

$$f(q) = f_{pc}(q) + ik \int_0^\infty db b J_0(qb) e^{-i\Phi_{pc}} \left( 1 - e^{i\Phi_N + i\delta\Phi_{uc}} \right), \quad (7)$$

where  $q = 2k \sin(\vartheta/2)$  is the transfer momentum,  $f_{pc}(q)$ , the known amplitude of scattering in the field of the Coulomb potential  $U_{pc} = Z_1 Z_2 e^2/r$ . Then,

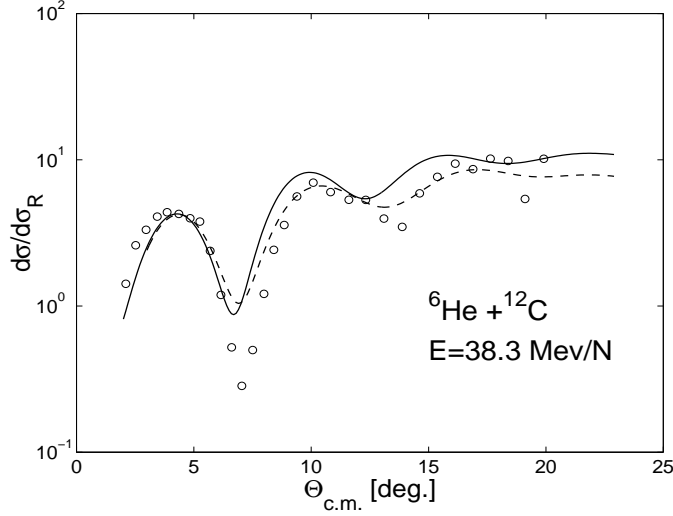


Figure 4. Differential cross sections of the  ${}^6\text{He}+{}^{12}\text{C}$  elastic scattering at  $E=38.3$  MeV/nucleon calculated for the same  $U_{opt} = (1.123 + i0.472) \cdot V^{DF}$  from [1] by using the eikonal method (solid curve) and the DWUCK4 code (dashed curve).

$\delta\Phi_{uc} = \Phi_{uc} - \Phi_{pc}$  is the difference of eikonal phases for the potential of a uniformly charged sphere and the  $U_{pc}$  potential, while the nuclear eikonal phase is

$$\Phi_N = -\frac{k}{E} \int_0^\infty U_{HeC}^{opt} \left( \sqrt{b^2 + z^2} \right) dz. \quad (8)$$

Note that when performing integration in (7) the trajectory distortion is taken into account by exchanging the impact parameter  $b$  by the distance of closest approach in the Coulomb field  $U_{pc}$  at  $b=0$ , i.e.  $b \rightarrow b_c = \bar{a} + \sqrt{\bar{a}^2 + b^2}$  with  $\bar{a} = Z_p Z_t e^2 / 2E_{c.m.}$ .

In Fig.4 is shown the comparison of two curves for  $d\sigma/d\sigma_R$  where  $d\sigma_R$  is the Rutherford cross section for scattering in the  $U_{pc}$  potential. The solid curve corresponds to the HEA method, and the dashed one is the exact DWUCK calculations. One can see that both curves coincide fairly well, especially at small angles, in the region that yields the main contribution to the total cross sections. Thus we conclude that the HEA method may be applied for our further estimations of the total breakup cross sections.

## 5 The HEA model for breakup reactions

The earlier HEA theory for the breakup processes were developed in refs. [11], [12] for investigations of stripping and dissociation of deuterons in nuclear col-

lisions. In recent papers (see, e.g., [13], [14] and refs therein) this method was generalized to study breakup reactions of lightest nuclei. For a brief review of this method we begin with the conditions  $E \gg |U|$ ,  $\vartheta \ll (1/kR)^{1/2}$  when the OP wave function of a high-energy particle can be considered in the eikonal form:

$$\Psi(\mathbf{r}) = e^{i\mathbf{k}\mathbf{r} - \frac{i}{\hbar v} \int_{-\infty}^z dz U^{opt}(\sqrt{b^2 + z^2})}, \quad (9)$$

After scattering at  $z \rightarrow +\infty$  this function becomes

$$\Psi(\mathbf{r}) = S(b) \cdot e^{i\mathbf{k}\mathbf{r}}, \quad S(b) = e^{-\frac{i}{\hbar v} \int_{-\infty}^{\infty} dz U^{opt}(\sqrt{b^2 + z^2})}, \quad (10)$$

where  $S(b)$  is an analog of the partial  $S_l$ -matrix, and formulae defined by  $S_l$  may be transformed to respective expressions with  $S(b)$  using relations  $l + 1/2 \rightarrow kb$  and  $(1/k) \sum_l \rightarrow \int db$ . So, after the collision the probability that the particle with an impact parameter  $b$  remains in the elastic channel is

$$|S_i(b)|^2 = e^{-\frac{2}{\hbar v} \int_0^{\infty} dz W_i(\sqrt{b^2 + z^2})}, \quad i = \alpha, h, \quad (11)$$

and the probability for the particle to be removed from the elastic channel is  $(1 - |S|^2)$ . (Here we denote  $W = |\text{Im}U|$ .) Thus, the common probability of both  $h$  and  $\alpha$  particles to leave the elastic channel is  $(1 - |S_h|^2)(1 - |S_\alpha|^2)$ . Then, one should average this latter by  $\varrho_b(s)$  that characterizes the probability of  $h$  and  $\alpha$  to be at relative distance  $s$ . As a result, for the  $h\alpha$ -model of  ${}^6\text{He}$  the total absorption cross section is obtained as follows

$$\sigma_{abs}^{tot} = 2\pi \int_0^{\infty} b_h db_h (1 - |S_h(b_h)|^2) (1 - I(b_h)), \quad (12)$$

where

$$I(b_h) = \int d^3s \varrho_b(s) |S_\alpha(b_\alpha)|^2, \quad b_\alpha = \sqrt{s^2 \sin^2 \vartheta + b_h^2 - 2sb_h \sin \vartheta \cos \phi} \quad (13)$$

Here the relation is used of impact parameters  $\mathbf{b}_\alpha = \mathbf{b}_h - \mathbf{b}$  with  $b = s \sin \vartheta$  being the projection of the  $h - \alpha$  vector  $\mathbf{s}$  on the plane normal to the  $Oz$ -axis along the straight line trajectory of an incident nucleus.

In the case of the stripping reaction with removing  $h$ -particle from  ${}^6\text{He}$  to the target nucleus, one should use the probability of  $h$  to leave the elastic channel  $(1 - |S_h(b_h)|^2)$ , and for  $\alpha$  to continue its elastic scattering with probability  $|S_\alpha(b_\alpha)|^2$ . Then the probability of the whole process is  $|S_\alpha(b_\alpha)|^2 \cdot (1 - |S_h(b_h)|^2)$ , and to get the total stripping cross section one must average over  $\varrho_b(s)$  as is done in (12),(13). In a similar manner the transfer of the  $\alpha$  particle can be constructed,

Table 2. The HEA estimations within the  $h\alpha$ -model of total cross sections of  ${}^6\text{He}+{}^{12}\text{C}$  at  $E=38.3$  MeV/nucleon.

potential	$\sigma_{abs}^{tot}$ , mb	$\sigma_{bu}^{tot}$ , mb	$\sigma_R^{tot}$ , mb
$ImOP=N_I W^{H(b)}$ , eq.(4), $N_I=1.7$	392	412	804
$ImOP=N_I V^{DF(b)}$ , eq.(3), $N_I=1.0$	447	389	830

and the net contribution of both removal reactions yields *the total breakup cross section*

$$\sigma_{bu}^{tot} = 2\pi \int_0^\infty b_h db_h \left\{ |S_h(b_h)|^2 + [1 - 2|S_h(b_h)|^2] \cdot I(b_h) \right\}. \quad (14)$$

The sum of the absorption (12) and breakup (14) cross sections results in *the total reaction cross section*

$$\sigma_R^{tot} = 2\pi \int_0^\infty b_h db_h \left( 1 - |S_h(b_h)|^2 \cdot I(b_h) \right) \quad (15)$$

## 6 Summary and conclusions

Estimations of the total cross sections were made with a help of the preliminary calculated imaginary parts of optical potentials  $U_h$  and  $U_\alpha$  for scattering of  $h$ - and  $\alpha$ -particles on  ${}^{12}\text{C}$ . Firstly, we treated them as the  $N_I W_{h,\alpha}^H$  potential done by eq.(4) of HEA, and also, in the other attempt, they were taken in the double-folding form  $N_I V^{DF}$  eq.(3) usually used for the real potentials. The re-normalization coefficients  $\{N_I\}$  are the same as they were fitted for the folded potentials (2) of the  $h\alpha$  model (Table 1, rows 2,3). Thereafter the respective probabilities of scattering  $|S_{h,\alpha}|^2$  (11) were obtained and applied in calculations of the respective cross sections (12),(14),(15) shown in Table 2. One can see that in this case the total reaction cross sections  $\sigma_R^{tot} = 804, 830$  mb turn out to be about 20% lower than those  $\sigma_R^{tot} = 1018, 1042$  mb obtained within the code DWUCK4 for the  $U_{HeC}^{(b)}$  optical potential (2), the result of folding the  $U_h$  and  $U_\alpha$  potentials with the  $h\alpha$ -density function  $\varrho_b(s)$ . This 20% difference seems not too large, but to get the more substantial conclusion one should make comparisons of results for folded OPs calculated not within the code DWUCK4 but using the eikonal expression for the total reaction cross section [11]

$$\sigma_R^{tot} = 2\pi \int_0^\infty b db \left\{ 1 - \exp \left[ -\frac{2}{\hbar v} \int_{-\infty}^\infty dz W \left( \sqrt{b^2 + z^2} \right) \right] \right\}. \quad (16)$$

One should underline that here it is involved only the imaginary parts  $W$  of the  $U_{HeC}^{(b)}$  optical potential (2), in our case they are  $W = 1.7W^H$  and  $W =$



$1.0V^{DF}$ . So, using (16) we got the respective reaction cross sections  $\sigma_R^{tot} = 952$  and  $965\text{ mb}$ . Thus, the difference of these results from the preceding HEA results  $\sigma_R^{tot} = 804$  and  $830\text{ mb}$  is only about 10%. The small rest discrepancy can arise due to the additional role of the real part of OP in the DWUCK calculations, while the HEA expression (16) depends only on the imaginary part of OP. The other effect is ought to the difference in formulae (15) and (16). Indeed, in the first one the density  $\rho_b$  folds in eq.(13) probability function  $|S_{h,\alpha}|^2$  having the bare potential  $W$  in the exponent. Otherwise, the cross section (16) contains the already folded potential in its exponent. By the way these effects occur to be not too significant, and one can conclude that the main mechanism of the absorption in elastic channel of the  ${}^6\text{He}+{}^{12}\text{C}$  scattering is ought to existence of the power dissociation channels of the  ${}^6\text{He}$  in two clusters  $h = 2n$  and  $\alpha$ .

**Acknowledgments.** The authors would like to thank Prof. A. Antonov and Prof. W. Scheid for helpful remarks and suggestions. The work was supported by the Program for collaboration of JINR and Bulgarian scientific centers. EVZ and KVL thank RFBR (grant No.09-01-00770) for partial financial support.

## References

- [1] V.K. Lukyanov, D.N. Kadrev, E.V. Zemlyanaya, A.N. Antonov, K.V. Lukyanov, and M.K. Gaidarov, *Phys. Rev. C* **82** (2010) 024604.
- [2] V. Lapoux, *e.a.*, *Phys. Rev. C* **66** (2002) 034608.
- [3] J.S. Al-Khalili, *e.a.*, *Phys. Lett. B* **378** (1996) 45.
- [4] V.K. Lukyanov, E.V. Zemlyanaya, and K.V. Lukyanov, JINR Preprint P4-2004-115, Dubna, 2004; *Phys. At. Nucl.* **69** (2006) 240.
- [5] D.T. Karataglidis, P.J. Dortmans, K. Amos and C. Bennhold, *Phys. Rev. C* **61** (2000) 024319.
- [6] D.T. Khoa and G.R. Satchler, *Nucl. Phys. A* **668** (2000) 3.
- [7] K.V. Lukyanov, Comm. JINR, P11-2007-38, Dubna, 2007.
- [8] V.K. Lukyanov, E.V. Zemlyanaya, and B. Słowiński, *Phys. At. Nucl.* **67** (2004) 1306.
- [9] P.D. Kunz and E. Rost, in *Computational Nuclear Physics*, edited by K. Langanke *et al.* (Springer-Verlag, New York, 1993), Vol.2, p.88.
- [10] V.K. Lukyanov and E.V. Zemlyanaya, *Int.J. Modern Phys. E* **10** (2001) 169.
- [11] R.J. Glauber, *Phys. Rev.* **99**, 1515 (1955); *ibid.* **100** (1955) 242.
- [12] A.I. Akhiezer and A.G. Sitenko, *Sci. Notes of Kharkov Univ.* **64** (1955) 9; *Phys. Rev.* **106** (1957) 1236.
- [13] K. Hencken, G. Bertsch, H. Esbensen, *Phys. Rev. C* **54** (1996) 3043.
- [14] C.A. Bertulani and P.G. Hansen, *Phys. Rev. C* **70** (2004) 034609.